Materials Transactions, Vol. 48, No. 6 (2007) pp. 1282 to 1287
Special Issue on Materials Science of Bulk Metallic Glasses-VII

Compositional Dependence of Thermal and Mechanical Properties of Quaternary Zr-Cu-Ni-Al Bulk Glassy Alloys

Yoshihiko Yokoyama[1] and Akihisa Inoue[2]

[1]*Advanced Research Center of Metallic Glasses, Institute for Materials Research, Tohoku University, Sendai 980-8577, Japan*
[2]*Tohoku University, Sendai 980-8577, Japan*

To determine the optimized composition of quaternary Zr-Cu-Ni-Al bulk glassy alloy, its thermal and mechanical properties are examined. Zr shows high correlation coefficients with T_g and Vickers hardness, whereas Ni and Al show high correlation coefficients with T_l and T_x, respectively. Only Cu shows no remarkable correlation coefficient with any thermal or mechanical properties. We conclude that a compositional region with a high (over 135 kJ/m^2) U-notch Charpy impact (CUE) value is located around the $Zr_{52}Cu_{30}Ni_8Al_{10}$ bulk glassy alloy, which exhibits a maximum CUE of 165 kJ/m^2. Moreover, a compositional region with high tensile strength (over 2000 MPa) is also located around the $Zr_{48}Cu_{32}Ni_8Al_{12}$ bulk glassy alloy, which shows a maximum tensile strength of 2100 MPa. [doi:10.2320/matertrans.MF200622]

(Received January 15, 2007; Accepted April 16, 2007; Published May 25, 2007)

Keywords: *zirconium-copper-nickel-aluminum quaternary alloy system, phase diagram, Vickers hardness, Young's modulus, tensile strength, Charpy impact value*

1. Introduction

Zr-based bulk glassy alloys were roughly classified into two groups by sp-electron element: Al[1)] and Be.[2)] We have been studying Zr-based bulk glassy alloys with Al element, because Be is regarded as poisonous. The principal alloy composition for Zr-TM-Al (TM: transition metals) bulk glassy alloy was identified in 1990[1)] and 1991.[3)] Many researchers have tried to determine the optimum composition, combining high glass-forming ability and superior thermal stability. The Zr-TM-Al bulk glassy alloys grew into a large group with many categorized functions. For example, the widest supercooled liquid region over 120 K was found in the Zr-Al-Cu-Ni-Co alloy[3)] system. Moreover, the additive Pd element for Zr-based glassy alloys improves glass formability[4)] and cast ability,[5)] which are necessary for continuous casting[6,7)] of $Zr_{60}Al_{10}Ni_{10}Cu_{15}Pd_5$ bulk glassy alloy. Especially, $Zr_{55}Cu_{30}Al_{10}Ni_5$ bulk glassy alloy enables the preparation of the largest cast sample–30 mm in diameter and 50 mm in length–using a suck-casting furnace.[8)] A plate-shaped squeeze-cast $Zr_{55}Cu_{20}Ni_{10}Al_{15}$ bulk glassy alloy shows a high tensile strength of about 1850 MPa,[9)] and $Zr_{55}Cu_{30}Ni_5Al_{10}$ bulk glassy alloy shows a high Charpy impact value of about 90 kJ/m^2.[10)] The $Zr_{55}Cu_{30}Al_{10}Ni_5$ bulk glassy alloy was also applied to golf clubs,[11)] whose composition is characterized by good balance along with high strength, high toughness, and a low Young's modulus even in a plate cast sample.

However, in Zr-Based bulk glassy alloys, increased oxygen absorption causes three significant problems: [1] decreased critical cooling rate of glass formation,[12)] [2] promotion of crystalline inclusion,[13)] and [3] significantly decreased toughness due to oxygen embrittlement.[14)] The oxygen embrittlement and reduced glass formability are considered fatal drawbacks for the industrial use of Zr-TM-Al bulk glassy alloys. These reports[12–14)] point out the risk of using sponge Zr material, because the oxygen concentration of sponge Zr metal varies widely, from 300 to 1,500 ppm. Further, the additive Ni, Pd, and Pt elements have been reported[15)] to improve oxygen embrittlement in Zr-TM-Al bulk glassy alloys. However, it is difficult to fabricate high-quality Zr-TM-Al bulk glassy alloys using common sponge Zr metal. Accordingly, we use a purified Zr metal called crystal Zr in the fabrication of Zr-based bulk glassy alloys to control low oxygen concentration less than 100 ppm. By using the crystal Zr, we were able to examine Zr-Cu-Al ternary phase diagrams[16)] to clarify the relationship between the glass-forming compositional area and the phase diagram. The compositional area with a low liquidus surface temperature is expanded along the binary eutectic line (L = τ_3 + Zr_2Cu) from the ternary eutectic point (L = Zr_2Cu + Zr-Cu + ZrCuAl). The τ_3 phase[17)] is often seen as crystalline inclusions in cast $Zr_{55}Cu_{30}Al_{10}Ni_5$ bulk glassy alloy with an insufficient cooling rate. The phase diagram shows that the optimum alloy composition to restrict the formation of crystalline inclusion is the ternary eutectic point Zr_{50}-$Cu_{40}Al_{10}$. However, an alloy composition with high glass forming ability is not usually very strong, tough, or thermally stable.

This paper presents the compositional dependence of the thermal and mechanical properties of quaternary Zr-Cu-Ni-Al bulk glassy alloys to optimize the composition for high strength or high toughness.

2. Experimental Procedure

Quaternary Zr-Cu-Ni-Al (Zr = 20–75 at%, Cu = 20–70 at% Ni = 0–15, and Al = 10–40 at%) alloys were examined in this study. Master alloy ingots were prepared by arc melting mixtures of pure Zr, Cu, Ni, and Al metals in an argon atmosphere. To avoid oxygen contamination, a special crystal Zr rod (<100 mass ppm oxygen) was used. The master alloy was completely remelted and cast into a rod shape (ϕ8 × 60 mm) by the arc-tilt casting method.[18)] Phase characterization of cast samples was performed by X-ray diffractometry and OM observation at a cross-sectional area

Table 1 Thermal and mechanical properties of cast Zr-Cu-Ni-Al bulk glassy alloys. T_l is liquidus surface temperature (K), T_g is glass transition temperature (K), T_x is crystallization temperature (K), CUE is U-notch Charpy impact value (kJm^{-2}), σ_B is tensile strength (MPa), HV is Vickers hardness, and E is Young's modulus (GPa).

Al %	Alloys	Thermal Properties			Mechanical Properties			
	alloy composition	T_l	T_x	T_g	σ_B	E	HV	CUE
12	$Zr_{44}Cu_{32}Ni_{12}Al_{12}$	1168	791	738	–	–	–	–
	$Zr_{44}Cu_{34}Ni_{10}Al_{12}$	1158	796	730	612	–	–	–
	$Zr_{46}Cu_{34}Ni_8Al_{12}$	1138	796	725	1777	111	562	110
	$Zr_{46}Cu_{30}Ni_{12}Al_{12}$	1144	790	733	1399	106	552	119
	$Zr_{48}Cu_{30}Ni_{10}Al_{12}$	1157	795	729	1472	107	544	117
	$Zr_{48}Cu_{28}Ni_{12}Al_{12}$	1160	789	725	1906	102	530	122
	$Zr_{48}Cu_{30}Ni_{10}Al_{12}$	1148	790	727	1980	92	528	105
	$Zr_{48}Cu_{32}Ni_8Al_{12}$	1110	804	715	2100	102	527	110
	$Zr_{48}Cu_{34}Ni_6Al_{12}$	1140	800	725	1899	94	529	109
	$Zr_{50}Cu_{26}Ni_{12}Al_{12}$	1106	793	712	1878	88	498	119
	$Zr_{50}Cu_{28}Ni_{10}Al_{12}$	1118	792	726	1993	92	517	124
	$Zr_{50}Cu_{30}Ni_8Al_{12}$	1123	794	723	1820	92	526	139
	$Zr_{50}Cu_{32}Ni_6Al_{12}$	1126	800	716	1875	92	521	134
	$Zr_{50}Cu_{34}Ni_4Al_{12}$	1118	804	714	1905	91	517	127
	$Zr_{52}Cu_{26}Ni_{10}Al_{12}$	1144	788	729	1960	89	509	125
	$Zr_{52}Cu_{28}Ni_8Al_{12}$	1107	796	716	1798	94	512	120
	$Zr_{52}Cu_{30}Ni_6Al_{12}$	1103	792	709	1820	93	506	134
	$Zr_{52}Cu_{32}Ni_4Al_{12}$	1118	792	703	1780	88	501	109
10	$Zr_{46}Cu_{30}Ni_{14}Al_{10}$	1179	779	736	–	–	551	25
	$Zr_{46}Cu_{32}Ni_{12}Al_{10}$	1170	780	732	–	–	530	47
	$Zr_{48}Cu_{30}Ni_{12}Al_{10}$	1164	778	726	1378	94	520	115
	$Zr_{48}Cu_{28}Ni_{14}Al_{10}$	1167	779	722	1560	91	518	103
	$Zr_{48}Cu_{32}Ni_{10}Al_{10}$	1151	780	722	1894	94	513	131
	$Zr_{50}Cu_{28}Ni_{12}Al_{10}$	1147	776	716	1809	89	518	110
	$Zr_{50}Cu_{32}Ni_8Al_{10}$	1133	781	717	1797	87	508	125
	$Zr_{50}Cu_{30}Ni_{10}Al_{10}$	1141	780	710	1963	92	509	129
	$Zr_{52}Cu_{32}Ni_6Al_{10}$	1122	784	694	1890	86	490	115
	$Zr_{52}Cu_{28}Ni_{10}Al_{10}$	1135	779	706	1892	88	498	109
	$Zr_{52}Cu_{30}Ni_8Al_{10}$	1123	781	713	1856	89	498	165
	$Zr_{54}Cu_{28}Ni_6Al_{10}$	1103	775	692	1780	83	477	125
	$Zr_{54}Cu_{28}Ni_8Al_{10}$	1114	778	695	1568	89	485	103
8	$Zr_{48}Cu_{36}Ni_8Al_8$	1167	767	702	1277	101	525	–
	$Zr_{48}Cu_{30}Ni_{14}Al_8$	1193	767	713	460	52	514	34
	$Zr_{48}Cu_{32}Ni_{12}Al_8$	1178	768	717	536	56	509	39
	$Zr_{48}Cu_{34}Ni_{10}Al_8$	1166	767	719	516	94	516	132
	$Zr_{50}Cu_{28}Ni_{14}Al_8$	1181	764	717	1800	86	509	105
	$Zr_{50}Cu_{30}Ni_{12}Al_8$	1166	764	712	296	71	507	83
	$Zr_{50}Cu_{32}Ni_{10}Al_8$	1179	766	708	1963	96	504	120
	$Zr_{50}Cu_{34}Ni_8Al_8$	1151	768	708	1888	98	503	132
	$Zr_{52}Cu_{28}Ni_{12}Al_8$	1167	765	697	1895	92	490	110
	$Zr_{52}Cu_{30}Ni_{10}Al_8$	1160	768	698	1828	84	490	97
	$Zr_{52}Cu_{32}Ni_8Al_8$	1135	770	703	1798	95	492	134
	$Zr_{52}Cu_{34}Ni_6Al_8$	1136	772	693	1864	92	488	117
	$Zr_{54}Cu_{30}Ni_8Al_8$	1107	765	694	1820	97	469	131
	$Zr_{54}Cu_{32}Ni_6Al_8$	1135	766	692	1805	97	475	132

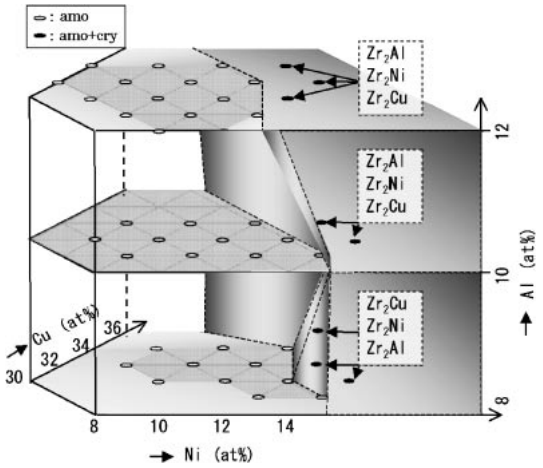

Fig. 1 Glass formation compositional area of cast Zr-Cu-Ni-Al bulk glassy alloys 8 mm in diameter and 60 mm in length. Open circle indicates the glass single phase, solid circle indicates the glassy phase with crystalline inclusions.

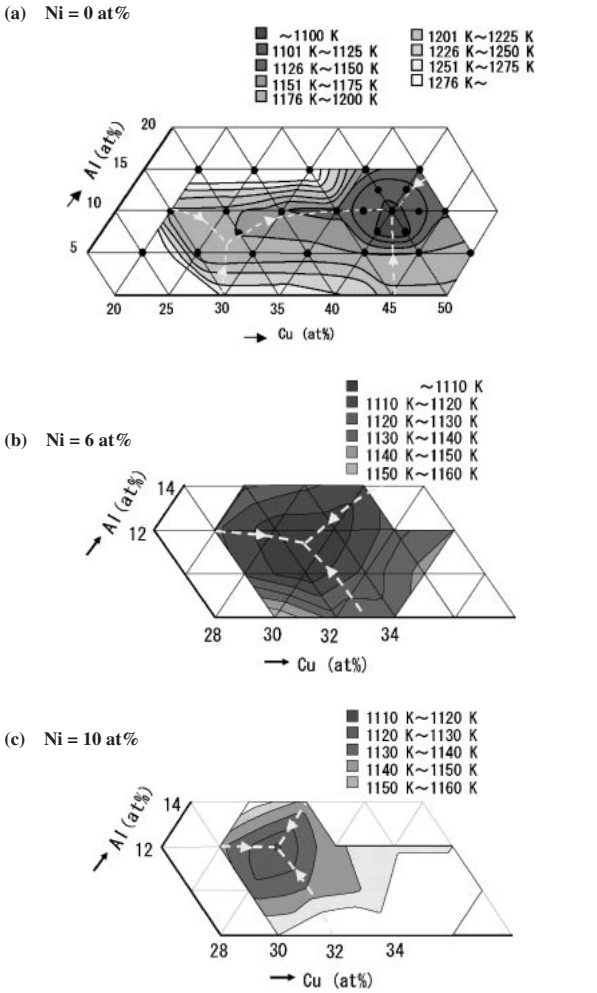

Fig. 2 Liquidus surface diagram of quaternary Zr-Cu-Ni-Al alloys with different Ni concentrations with Ni = 0 at% (a), Ni = 6 at%, and Ni = 10 at%, respectively.

from the topside of the cast sample. We measured the oxygen concentrations of cast samples by fusion in the helium gas-infrared absorption method. The liquidus surface temperatures of the samples were measured by differential thermal analysis (DTA) under a low cooling rate (1.6×10^{-2} K/s) from the completely melted state in an argon atmosphere. In addition, we measured the samples' glass-transition and crystallization temperatures by differential scanning calorimetry (DSC) under heating (0.67 K/s) in an argon atmosphere. We measured the tensile strength, tensile fracture strain, and Young's modulus using an Instron 5582 testing machine. A Charpy impact test was also performed in dry air using half-height samples with a size of $55 \times 10 \times 5$ mm, which were U-notched to 2 mm in depth.

3. Results and Discussion

Quaternary Zr-Cu-Ni-Al bulk glassy alloy is used popularly in structural materials due to its high strength and high toughness. However, there is not enough data to determine the alloy composition of Zr-Cu-Ni-Al bulk glassy alloys that have desired mechanical properties. We examined the thermal and mechanical properties of cast Zr-Cu-Ni-Al bulk glassy alloys with a wide compositional range and summarize the data in Table 1. The samples, each of which shows an extremely low Young's modulus or no tensile strength, indicate the existence of crystalline inclusions due to insufficient glass forming ability for bulk cast samples 8 mm in diameter and 60 mm in length.

Figure 1 shows the compositional range of a single glassy phase and the types of crystalline inclusions in cast Zr-Cu-Ni-Al alloys. There is a wide formation area of the single glassy phase in bulk-shaped Zr-Cu-Ni-Al alloys. The widest compositional range of Cu and Ni elements is observed in Al = 10 at% condition. We also examined the phase diagram in a quaternary Zr-Cu-Ni-Al alloy system with fixed Ni concentrations at 0, 6, and 10 at%, revealing distinct changes in the phase diagram. Figure 2(a) shows the partial ternary liquidus surface phase diagram of the Zr-Cu-Al alloy system. Figure 2(b) and (c) show a pseudoternary liquidus surface phase diagram with Ni = 6 and 10 at%, respectively. The ternary/pseudoternary eutectic point shifts to a Zr-enriched composition with Ni concentration. The temperature of the ternary/pseudoternary eutectic point increases monotonically with Ni concentration.

If a bulk glassy alloy shows little plastic deformability, the fracture toughness originates mainly in stored elastic strain energy. However, the fracture toughness of ductile bulk glassy alloy, which shows sufficient plastic deformability under bending or compressing, can be significantly enhanced by local plastic deformation, with the formation and blanching of shear bands in front of the crack tip to relax localized stress. Consequently, fracture toughness is strongly influenced by the shear band forming and blanching abilities. The optimized compositions with high strength and high ductility might be different. Figure 3 shows the compositional dependence of the tensile strength of tilt-cast Zr-Cu-Ni-Al bulk glassy alloys and illustrates the compositional region that has high (over 2000 MPa) tensile strength. The compositional region is located around the $Zr_{48}Cu_{32}Ni_8Al_{12}$ bulk glassy alloy, which exhibits the highest tensile strength, 2100 MPa. Moreover, the tensile strength decreases signifi-

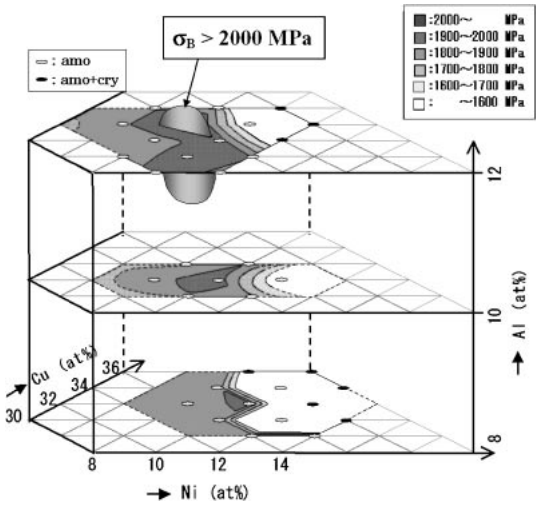

Fig. 3 Compositional dependence of tensile strength of cast Zr-Cu-Ni-Al bulk glassy alloys.

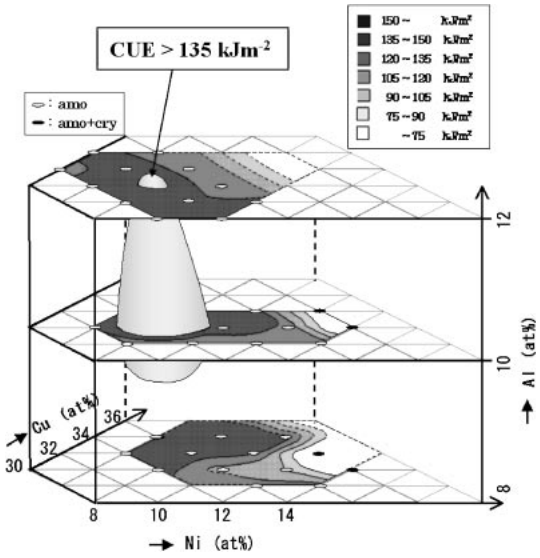

Fig. 4 Compositional dependence of U-notch Charpy impact value of cast Zr-Cu-Ni-Al bulk glassy alloys.

cantly with the crystallization-induced increase of solute Cu and Ni. Therefore, the strengthening bulk glassy alloy occurs near the edge of the glass-formation compositional region to form the typical chemical short-range order as strong atomic bond networks in the glass structure. Figure 4 shows the compositional dependence of U-notch Charpy impact energy (CUE) of tilt-cast Zr-Cu-Ni-Al bulk glassy alloys, and it illustrates the compositional region with high (over 135 kJm^{-2}) CUE. The compositional region is located around the $Zr_{52}Cu_{30}Ni_8Al_{10}$ bulk glassy alloy, which exhibits the highest CUE value, 165 kJm^{-2}. The compositional region with high strength (over 2000 MPa) is located in a solute enriched composition from the compositional region with a high CUE (over 135 kJm^{-2}).

To clarify the role of each element in Zr-Cu-Ni-Al bulk glassy alloys, we evaluate the correlation coefficients between the element's concentration and thermal/mechanical properties. Figure 5(a) shows the relationship between the Zr concentration and Vickers hardness. A clear negative proportionality relation can be seen with a high correlation coefficient, −0.88. Figure 5(b) shows the relationship between Zr concentration and glass transition temperature; here, too, we can see a clear negative proportionality relation with a high correlation coefficient, −0.82. Therefore, since the Zr-enriched glassy alloys exhibit softening, the Zr element degrades the alloy's stiffness. Figure 6(a) shows the relationship between the Ni concentration and CUE. CUE is not dependent on the Ni concentration, whereas the maximum CUE is obtained at 8 at% Ni and crystallization can be seen over 12 at% Ni. The maximum CUE value is obtained in $Zr_{52}Cu_{30}Ni_8Al_{10}$ bulk glassy alloy at 165 kJm^{-2}. On the other hand, additional Ni element has a positive proportionality relation to the liquidus surface temperature, as shown in Fig. 6(b). Additive Ni elements probably cause a typical strong chemical short-range order to increase the melting temperature. The Al concentration has a close positive proportionality relation to crystallization temperature, as shown in Fig. 7, with high correlation coefficient, 0.96. Since the crystallization temperature is decided by the type of crystalline, the Al concentration causes the systematic change in the crystalline phase under heating.

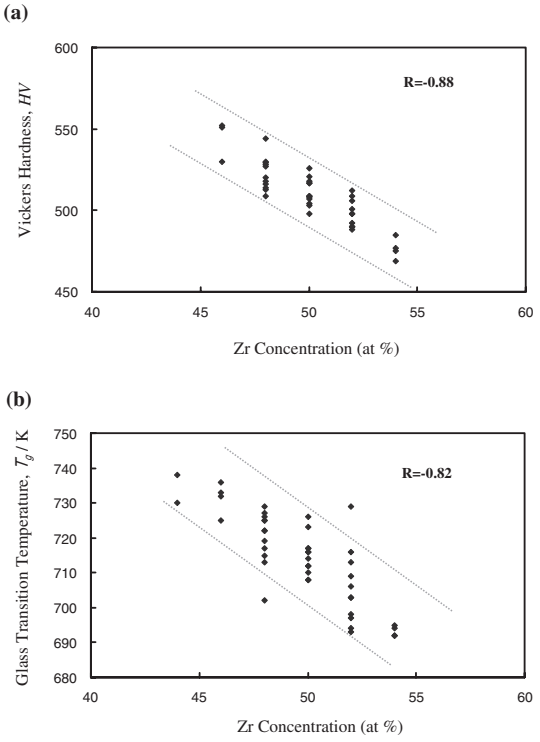

Fig. 5 Relationship between the Zr concentration and U-notch Charpy impact value: CUE (a), and relationship between the Zr concentration and glass transition temperature: T_g (b) of cast Zr-Cu-Ni-Al bulk glassy alloys.

Table 2 shows the correlation coefficient between each element's concentration and properties. It is guessed that two properties with a high correlation coefficient are intrinsic properties, because both properties originate in the same structural or bond state change in bulk glassy alloy. A noteworthy point for this table is that Cu has no high correlation coefficient with any thermal or mechanical

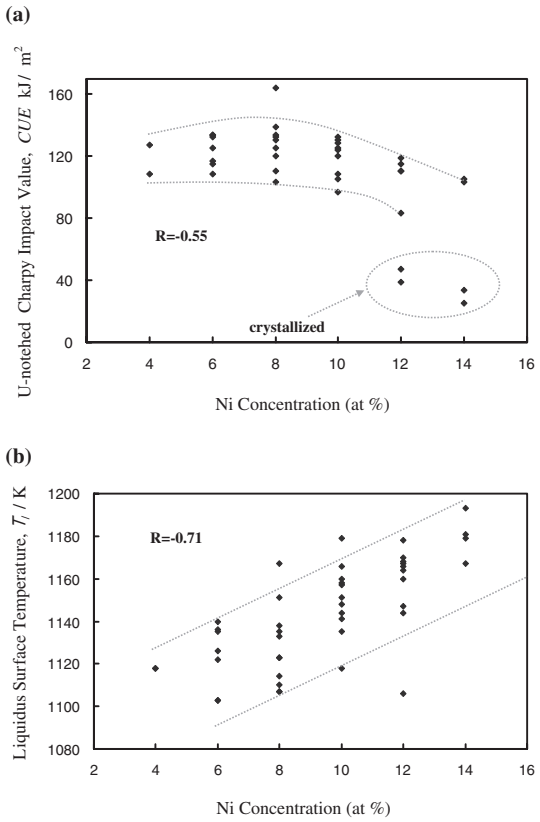

Fig. 6 Relationship between the Ni concentration and Vickers hardness: HV (a), and relationship between the Zr concentration and liquidus surface temperature: T_l (b) of cast Zr-Cu-Ni-Al bulk glassy alloys.

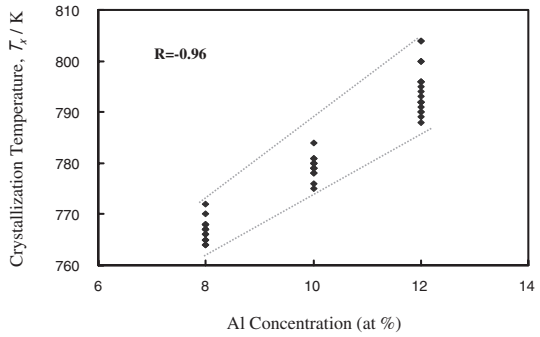

Fig. 7 Relationship between the Al concentration and crystallization temperature: T_X of cast Zr-Cu-Ni-Al bulk glassy alloys.

Table 2 The correlation coefficient between the element concentration and the thermal and mechanical factors of cast Zr-Cu-Ni-Al bulk glassy alloys. T_l is liquidus surface temperature (K), T_g is glass transition temperature (K), T_x is crystallization temperature (K), CUE is U-notch Charpy impact value (kJm^{-2}), σ_B is tensile strength (MPa), HV is Vickers hardness, and E is Young's modulus (GPa).

Properties		Zr	Cu	Ni	Al
Thermal	T_l	−0.56	0.12	0.71	−0.45
	T_x	−0.30	0.01	−0.32	0.96
	T_g	−0.82	−0.06	0.49	0.55
Mechanical	σ_B	0.43	−0.30	−0.38	0.37
	E	−0.05	0.02	−0.44	0.49
	HV	−0.88	0.01	0.39	0.52
	CUE	0.38	−0.04	−0.43	0.28

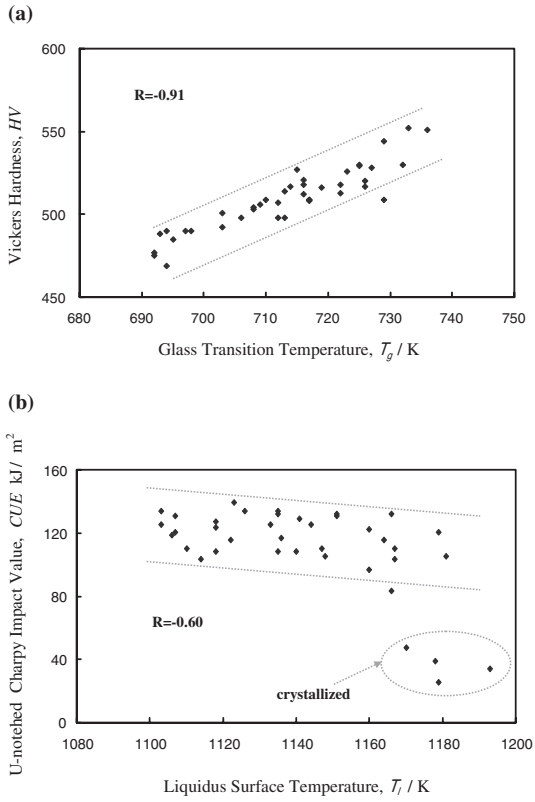

Fig. 8

properties. This implies that the Cu element in the glass structure is regarded as a no-individuality element, which can be easily replaced by other elements. Moreover, Cu can also behave like Zr, Ni, or Al in bulk glassy alloy, whereas the compositional range should be limited around the pseudoternary eutectic point. The Cu element, which does not have strong individuality in bulk glassy alloy, has an important role in maintaining the liquid/glass structure during the freezing of molten alloy. Since Cu elements in bulk glassy alloy are easily exchangeable with Zr, Al, and Ni elements, vitrification during solidification is also possible if there is insufficient redistribution time to stabilize the random structure. Therefore, we consider that the high glass-forming ability of Zr-Cu-Ni-Al bulk glassy alloys derives from the unique character of the Cu element in glassy alloy. Zr is the base element of the glassy alloys, and excessive Zr promotes the decrease in stiffness due to the declining number of strong bonds such as Zr-Al and Zr-Cu/Ni. In a certain sense, Al may be a key element to form the backbone structure of bulk glassy alloy by its anisotropic and strong bond with Zr, and it shows high solubility against Ni and Cu elements.

4. Summary

We examined the compositional dependence of the thermal and mechanical properties of quaternary Zr-Cu-Ni-Al bulk glassy alloys to determine the roles of several elements. The results are summarized as follows.

(1) Zr has large correlation coefficients with T_g and Vickers hardness. Ni and Al have high correlation coefficients with T_l and T_x, respectively. Only the Cu exhibits no remarkable composition dependability of thermal or mechanical properties.
(2) The compositional region with high (over 2000 MPa) tensile strength is localized around the $Zr_{48}Cu_{32}Ni_8Al_{12}$ bulk glassy alloy, which shows the highest tensile strength, 2100 MPa.
(3) The compositional region with high (over 135 kJm^{-2}) U-notch Charpy impact energy (CUE) is located around the $Zr_{52}Cu_{30}Ni_8Al_{10}$ bulk glassy alloy, which shows the highest CUE, 165 kJm^{-2}.

Acknowledgements

The authors are grateful to Mr. Atsushi Kobayashi, who was a graduate student at the Himeji Institute of Technology, for his support with the experiments. This research was funded in part by Grant-in-Aid for Scientific Research on Priority Area (Materials Science of Bulk Metallic Glasses) from the Ministry of Education, Culture, Sports, Science and Technology and NEDO (the New Energy and Industrial Technology Development Organization).

REFERENCES

1) A. Inoue, T. Zhang and T. Masumoto: Mater. Trans. **31** (1990) 177–183.
2) A. Pecker and W. L. Johnson: Appl. Phys. Lett. **63** (1993) 2342–2344.
3) T. Zhang, A. Inoue and T. Masumoto: Mater. Trans. **32** (1991) 1005–1010.
4) A. Inoue, T. Shibata and T. Zhang: Mater. Trans. **36** (1995) 1420–1426.
5) A. Inoue, Y. Shinohara, Y. Yokoyama and T. Masumoto: Mater. Trans. **36** (1995) 1276–1281.
6) A. Inoue, Y. Yokoyama, Y. Shinohara and T. Masumoto: Mater. Trans. **35** (1994) 923–926.
7) Y. Yokoyama and A. Inoue: Mater. Trans. **36** (1995) 1398–1402.
8) A. Inoue and T. Zhang: Mater. Trans. **37** (1996) 185–187.
9) T. Zhang and A. Inoue: Mater. Trans. **39** (1998) 1230–1237.
10) A. Inoue and T. Zhang: Mater. Trans. **37** (1996) 1726–1729.
11) H. Kakiuchi, A. Inoue, M. Onuki, Y. Takano and T. Yamaguchi: Mater. Trans. **42** (2001) 678–681.
12) X. H. Lin, W. L. Johnson and W. K. Rhim: Mater. Trans. **41** (2000) 1530–1537.
13) A. Gebert, J. Eckert and L. Schultz: Acta Mater. **46** (1998) 5475–5482.
14) Y. Yokoyama, A. Kobayashi, K. Fukaura and A. Inoue: Mater. Trans. **43** (2002) 575–579.
15) Y. Yokoyama, K. Fukaura and A. Inoue: Mater. Sci. & Eng. **A375–377** (2004) 427–431.
16) Y. Yokoyama, H. Inoue, K. Fukaura and A. Inoue: Mater. Trans. **43** (2002) 571–574.
17) Y. Yokoyama, T. Shinohara, K. Fukaura and A. Inoue: Mater. Trans. **45** (2004) 1819–1823.
18) Y. Yokoyama, K. Inoue and K. Fukaura: Mater. Trans. **43** (2002) 2316–2319.